Int. J. Sci. R. Tech., 2024 1(11)
A Multidisciplinary peer-reviewed Journal
www.ijsrtjournal.com [ISSN: 2394-7063]

Original Article

In-Depth In-Silico Functional, And Structural Screening Of *IL-4* Gene Variants Linked with Pink Eye Infection

Hamna Tariq[1*], Aniqa Amir[1], Muhammad Saleem[1], Kainat Ramzan[2*], Tuba Aslam[1], Mehmooda Asif[1]

[1]*Department of Molecular Biology, University of Okara, Punjab, 53600, Pakistan.*
[2]*Department of Biochemistry, Faculty of Life Science, University of Okara, Punjab, 53600, Pakistan.*

ABSTRACT

Conjunctival inflammation affects millions globally and can be triggered by microbial infections, allergens, or genetic factors. This study focuses on specific SNPs in the IL-4 gene, linked to pink eye susceptibility. Using *In-Silico* tools, 15 SNPs were identified as potentially damaging to IL-4 protein, with the R139G, A118G, R112C, and R139W variants showing probable damage on high RMSD values, as highlighted by SAVESV6.1. Structural analysis using HOPE predicted that the R139W mutation may be structurally bigger than the IL-4 wild type, while other variants were damaging to protein stability and function. Molecular docking studies with PyRx screened 25 small molecules for interactions with IL-4. Compounds such as Ioniflavone, Meridine, Palbociclib, Pyranoamentoflavone, Ramipril, and Tetracycline demonstrated strong binding affinities with IL-4, suggesting potential therapeutic efficacy. Visualization through Discovery Studio revealed differences in residue interactions, hydrogen bonds, and hydrophilic interactions between the wild-type and mutant forms, indicating that these SNPs could alter IL-4 structure and binding. These findings suggest that genetic variants in IL-4 may play a role in pink eye susceptibility and open avenues for developing targeted therapies. Their potential in targeting IL-4-related pathways further supports their use in addressing the immune component of conjunctivitis. However, each compound would require further clinical and pharmacological evaluation to confirm efficacy and safety for ophthalmic use. Further laboratory and clinical studies are essential to validate these results and explore personalized treatments for pink eye based on IL-4 genetic profiles.

Keywords: IL-4, SNPs, PPh2, SIFT, PANTHER.

INTRODUCTION

Interleukin-4 (IL-4) is a type I pleiotropic cytokine known for its four-α-helical bundle structure and its wide-ranging effects on different cell types, which is significant in both the innate and adaptive immune responses. Initially, B and T cells were identified as the primary targets affected by IL-4, highlighting its significance in immune regulation. In 1982, IL-4 was first discovered by Ellen Vitetta and her research team, with additional contributions by Maureen Howard and William E. Paul, who also helped characterize its functions [1]. In humoral immunity, it directs B-cells to produce IgE while inhibiting Th1 cytokines (IFN-gamma and IL-2). This change highlights the significance IL-4 is for fostering a Th2-mediated, antibody-focused response, which is required for controlling extracellular infections and allergy responses [2]. The IL-4 receptor is widely distributed across various organs, including the brain, fibroblasts, endothelial cells, epithelial cells, muscles, and liver, where it regulates immune functions. Genetic mutations in IL-4 and IL-4R genes can alter protein expression and activity, potentially influencing susceptibility or resistance to infectious diseases, rheumatoid arthritis, asthma, and atopy [3]. Elevated IL-4 levels are observed in seasonal allergic conjunctivitis patients and vernal keratoconjunctivitis, underscoring its significant role in these allergic eye conditions [4]. Conjunctival inflammation is frequently brought on by infections, allergies, or irritants, resulting in pink eye (conjunctivitis), which is characterized by redness in the eyes. Ocular discomfort, impaired vision, and light sensitivity are among the symptoms. Adenoviruses are frequently responsible for viral conjunctivitis [5], and are accompanied by fever, lymphadenopathy (especially preauricular), pharyngitis, and upper respiratory tract infections [6]. Moreover, common microbes responsible for bacterial conjunctivitis include *Staphylococcus*

Relevant conflicts of interest/financial disclosures: The authors declare that the research was conducted in the absence of any commercial or financial relationships that could be construed as a potential conflict of interest.

pneumoniae, Haemophilus influenzae, and *Moraxella catarrhalis*. Among these, *H. influenzae*, particularly non-typeable strains accounting for about 70% of cases [7] . Common signs of bacterial conjunctivitis include red eyes and a thick, mucopurulent discharge, often green or yellow [8]. Allergic conjunctivitis is a hypersensitivity reaction triggered by airborne allergens like pollen, dander, dust, and mold. It occurs when mast cells degranulate in response to an IgE-mediated reaction, releasing histamine and other inflammatory mediators. This condition peaks in young people between the ages of 15 and 18, affecting about 20% of them [9]. Similar to viral conjunctivitis, allergic conjunctivitis may show a follicular appearance of the tarsal conjunctiva, characterized by small bumps or nodules on the inner eyelid surface, along with watery discharge during clinical examination [10] Allergic conjunctivitis may not always show the typical symptoms, while blepharitis and meibomian gland dysfunction can present eye irritation and discomfort [11]. The IL-4 promotes the differentiation of naive T cells into Th2 cells, which boosts the production of immunoglobulin E (IgE) and other cytokines that drive allergic reactions and inflammation in the conjunctiva [12].

The IL-4 gene is located on human chromosome 5q31-q33 region and comprises 4 exons and 3 introns, with the exons encoding its functional domains. It is primarily produced by activated T cells, mast cells, basophils, and eosinophils that promote Th2 cell differentiation and stimulate B cell proliferation and class switching to IgE, playing a key role in humoral immunity and allergic responses. Immune responses and vulnerability to infections can be impacted by variations in the IL-4 gene [13]. The c.-589C>T (rs2243250) is located in the IL4 promoter region and shows notable differences in frequency between patients with viral conjunctivitis and healthy individuals [14]. The presence of the T allele may increase susceptibility to viral infections by altering IL-4 expression, potentially compromising immune responses [3]. The IL-4R variant rs1805010 (c.223A>G) was also analyzed for viral conjunctivitis, but no significant differences in its frequency were observed between affected patients and healthy controls [14].

It regulates B cell differentiation into plasma cells and promotes the proliferation of T and B cells. It induces B cells to switch to IgE production and enhances MHC class II expression. The IL-4 exposure also reduces the IL12 production, IFNγ, and macrophages by dendritic cells and elevated IL-4 levels can lead to the development of allergic reactions [15]. In extravascular tissues, IL-4 promotes the activation of macrophages into M2 cells, which aid in tissue repair and immune regulation, while inhibiting M1 cells, which are involved in inflammation and host defense. Pathological inflammation decreases as M2 macrophages and the release of IL-10 and TGF-β increase, activated M2 cells produce substances (arginase, proline, polyamines, and TGF-β) that are major contributors to wound healing and fibrosis [16]. Furthermore, IL-4 variants significantly impact human health by influencing immune responses related to eye infections, particularly viral conjunctivitis. This study explored the *IL-4* protein using several bioinformatics approaches to predict pathogenic coding variants and evaluate their potential effects on disease. We performed a functional analysis to assess the variant's impact on protein stability and function. The 3D structure of IL-4 was predicted, and we analyzed the conformational changes caused by mutations. Additionally, blind docking studies were conducted to investigate Protein-Ligand interactions, and the results were visualized to assess binding affinities and potential mechanisms. This comprehensive approach enhances our understanding of IL-4 role in pink eye disease.

1. Methodology

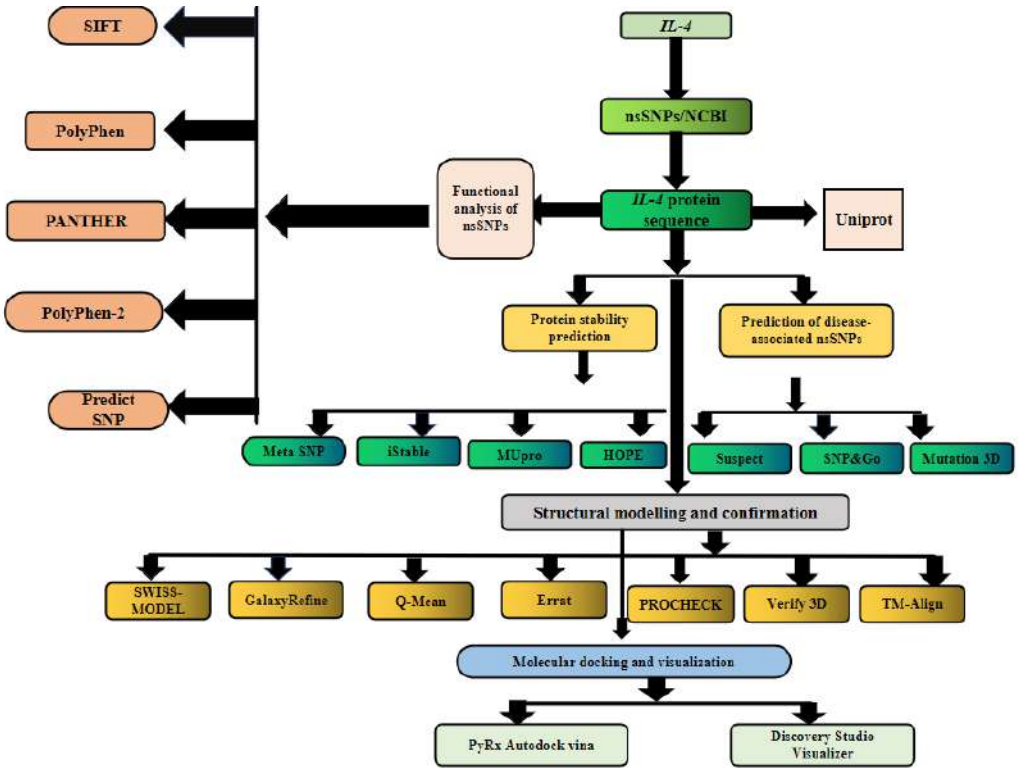

Figure 1. Schematic study of the complete overflow of the current study

2.1. Variant collection

We collected data on the human *IL-4* gene from the National Center for Biotechnology Information (NCBI) (https://www.ncbi), GnomAD (https://gnomad.broadinstitute.org), Ensembl (http://asia.ensembl.org/Homo_sapiens/Gene/Summary), and the NCBI dbSNP database, which provided information on IL-4 gene variants. UniProtKB (http://www.uniprot.org/uniprot) was used to acquire the protein sequence in FASTA format. A schematic overview of the study workflow is provided in **Figure 1**.

2.2. Functional analysis of coding *IL-4 variants*

2.2.1. SNPnexus

We employed SNPnexus (https://www.snp-nexus.org) for functional predictions of IL-4 gene variants. The tool utilized rsIDs extracted from the dbSNP database as query inputs to assess the potential functional impacts of specific SNPs [17]. Sorting Intolerant from Tolerant (SIFT) tool based on sequence homology, evaluates mutation impacts on protein function. Mutations with a SIFT score of < 0.05 are predicted to be detrimental, while those with a score >0.05 are considered tolerable [18]. Polymorphism Phenotyping (PolyPhen) evaluates these variants based on structural data or a combination of sequence and structural information to predict their impact on protein function [18].

2.2.2. Polymorphism Phenotyping V2

PolyPhen-2 (http://genetics.bwh.harvard.edu/pph2) played a crucial role in our investigation, enabling us to predict the potential implications of amino acid changes on protein structure and function. We entered our protein sequence, database ID/accession number, and details on amino acid changes into the server. Additionally, it provides a count score, with a value of 1 indicating the probable damage, along with predictions about the potential impact of missense variants on protein function [19].

2.2.3. Protein Analysis through Evolutionary relationship

PANTHER (http://pantherdb.org/tools/csnpScoreForm.jsp) predicts the functional impact of missense variants based on molecular activities, protein interactions, and evolutionary relationships. It calculates position-specific evolutionary conservation (PSEC) scores by aligning related proteins in structure and evolution. The prediction is based on the protein sequence and amino acid changes. The results are classified into three categories, probably damaging, possibly damaging, or probably benign based on evolutionary time and protein alignment data [20].

2.2.4. PredictSNP

PredictSNP (https://loschmidt.chemi.muni.cz/predictsnp1) combines data from multiple sources to predict the impact of a single amino acid change. By integrating

various tools, it provides a more efficient and accurate consensus prediction compared to individual prediction methods [21].

2.3. Association of disease-causing SNPs

2.3.1. Single nucleotide polymorphism & Gene Ontology

SNPs & GO (https://snps.biofold.org/snps-and-go/snps-and-go.html) uses a novel framework to predict whether a mutation is associated with disease, integrating genetic data, protein sequence, and Gene Ontology (GO) terms, along with 3D structural information. The tool classifies mutations as disease-associated if the probability score >0.5, and neutral < 0.5 while input files include FASTA sequences and protein variants [22].

2.3.2. Meta-SNP

Meta SNP (https://snps.biofold.org/meta-snp) is a meta-predictor that uses a random forest method to classify mutations as either 'Disease' or 'Neutral.' It is designed to detect disease-causing single nucleotide variations (nsSNVs), offering the potential for early detection and classification of harmful genetic variations, which is a promising development in genomics [23].

2.3.3. SuSPect

SuSPect (http://www.sbg.bio.ic.ac.uk/suspect) combines annotation and sequence-based approaches to prioritize disease-candidate genes. By leveraging multiple lines of evidence, it enhances performance in scoring genes quickly and efficiently, while minimizing the impact of annotation bias, making it a valuable tool in genomic research for identifying disease-related genes [24].

2.4. Consequences of nsSNP on Protein Stability

2.4.1. iStable

The iStable server (http://predictor.nchu.edu.tw/iStable) predicts changes in protein stability by using either sequence or structure information as input. It integrates results from five different prediction tools, combining various methods developed by different teams to offer a more comprehensive and accurate assessment of potential changes in protein stability [25].

2.4.2. MUpro

The MUpro server (http://mupro.proteomics.ics.uci.edu) predicts the impact of single-site mutations on protein stability using machine learning tools, including neural networks and support vector machines. MUpro predictions provide the energy change (DDG), the direction of that change, and a confidence score (ranging from -1 to 1) to indicate the accuracy of the stability prediction [26].

2.5. Structural Integration of IL4

2.5.1. IL4 template prediction

The SWISS-MODEL server (https://swissmodel.expasy.org) predicts protein 3D structures using sequence data. By submitting a FASTA sequence, the server aligns it with templates from the UniProtKB proteome to generate a model. The quality of the resulting structure is assessed using various metrics, such as the Ramachandran Plot, the QMEAN score and the MolProbity score. Moreover, the server provides annotations with experimental data, enabling researchers to select the most reliable model for further analysis [27].

2.5.2. Model Validation and refinement

The QMEAN method (https://swissmodel.expasy.org/qmean/help) tool was used for qualitative model energy analysis. It evaluates the quality of protein models by comparing their z-scores to reference structures of similar size in the Protein Data Bank (PDB). This clustering-based approach provides an empirical solution, helping to assess the reliability of models by structural properties and their alignment with known reference data [28]. The 3D protein models were further assessed using the Structure Validation Server v6.1 (https://saves.mbi.ucla.edu), which provided an evaluation of the model's z-score and identified potential structural defects. This server offers a detailed analysis, helping to confirm the accuracy and stability of the selected model by highlighting any issues that could impact its reliability [29].

2.5.3. Template modeling alignment

The TM-align (https://zhanggroup.org/TM-align) is used to compare native and mutant protein structures by performing a residual-residual alignment. The comparison is quantified using the TM-score, which ranges between 0 and 1, and the RMSD (Root Mean Square Deviation), which measures the variation between the native and mutated structures. The TM-score indicates the structural similarity (1 represents perfect match), while the RMSD reflects the degree of variation or deviation between the two structures [30]. PyMOL (https://pymol.org) is assessed for visualizing, analyzing, and manipulating predicted

residues and evolutionary sites in protein structure [31].

2.6. Blind protein-ligand docking studies

2.6.1. Ligand Selection

The gene sequences obtained from UniProtKB for the proteins are consistent, ensuring a reliable source for further bioinformatics analysis. The PubChem IDs of the pharmaceutical compounds used in this study were sourced from the ZINC database (https://zinc.docking.org) and PubChem (http://www.ncbi.nlm.nih.gov/pccompound). These compounds were then converted into PDB format using the Discovery Studio v4.1 (https://discover.3ds.com/discovery-studio-visualizer-download) and the academic edition of PyMol (https://pymol.org) [32, 33].

2.6.2. PyRx 0.8 Program

The docking experiments were carried out using the freely accessible PyRx 0.8 program (https://pyrx.sourceforge.io). The process began by loading a protein in PDB format and converting it into a macromolecule. A ligand was selected and transformed using the AutoDock button. The Vina Wizard was launched by clicking the start button, followed by setting up the grid with the "maximize" option. Vina was activated by pressing the appropriate button. After sufficient time, the best docking scores for each protein-ligand pair were recorded. To analyze the ligand-protein interactions, the Discovery Studio Visualizer was used to generate 2D and 3D PNG images of the ligand and protein [34, 35].

2.7. Structural Analysis of Variants

The Mutation 3D tool (http://www.mutation3d.org) was utilized to visualize and investigate the spatial distribution of amino acid alterations on protein structures and model [36]. The HOPE Project (http://www.cmbi.ru.nl/hope/input) is a comprehensive tool designed to forecast the physical and chemical properties of proteins, and their function, hydrophobicity, and spatial structure. Users can input a single identification, such as UniProt ID, Gene/Protein Symbol, or Ensemble Transcript, into its interface [37].

3. RESULTS

3.1. Datasets

The variations in the human IL-4 gene were sourced from NCBI dbSNP, Ensembl, and GnomAD databases. **Figure 2** categorizes single nucleotide polymorphism (SNP) distribution within the IL-4 gene, highlighting key genomic regions. The 3′ UTR region contains 97 SNPs, and the broader UTR region has 125 SNPs. Within two distinct intronic regions, 5,133 SNPs are found in one, and 1,140 in the other. The coding region includes 5,616 SNPs, divided into 97 exonic, 323 missense, and 160 synonymous SNPs. Additionally, there are 1,237 SNPs in non-coding regions. The 3′ downstream region contains 977 SNPs, while the 5′ upstream region has 775 SNPs, including 28 SNPs within the 5′ UTR. This detailed classification offers a comprehensive view of SNP distribution across the IL-4 gene. The missense nsSNPs were chosen for further investigation, as these variants are more likely to impact protein function by causing amino acid changes, potentially altering the structure, stability, or function of the IL-4 protein. This selection focuses on identifying variations with a higher probability of functional relevance, which may provide insights into the gene's role in disease mechanisms.

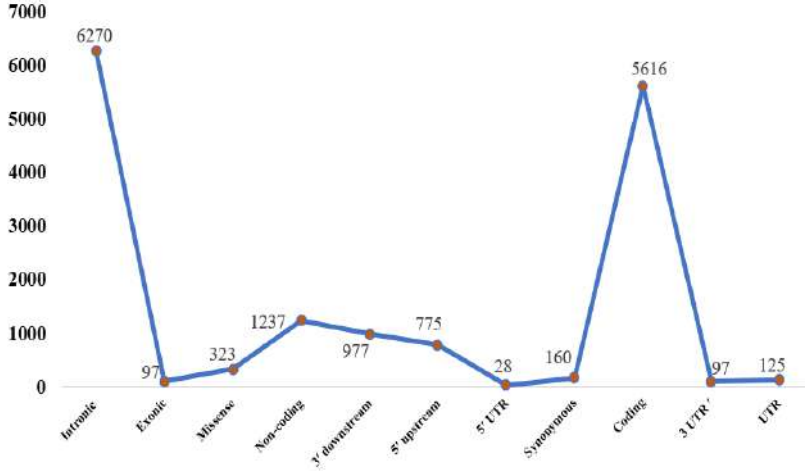

Figure 2. The prediction of variations is categorized into key genomic regions of IL4.

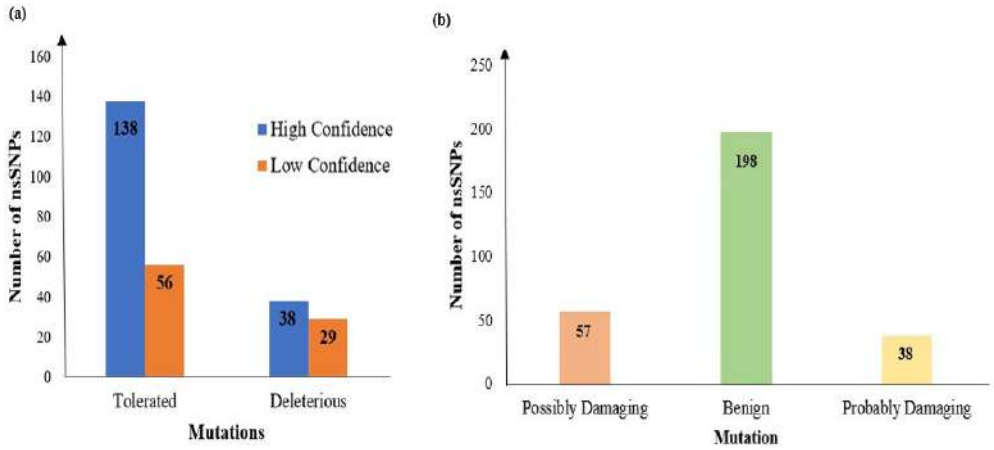

Figure 3. Bar plot of SNPs identified by a) SIFT and b) PolyPhen.

3.2. Deleterious nsSNPs *In-Silico* prediction

Using sequence homology of amino acids, SIFT provided predictions for a set of identified nsSNPs by revealing 261 nsSNPs as frequent, with 194 deletions projected to be deleterious and 67 deemed tolerable. PolyPhen results predicted that 57 nsSNPs were likely damaging, 38 possibly damaging, and 198 benign, as shown in **Figure 3**. Among these, 15 SNPs were identified as highly deleterious and selected for in-depth analysis as given in **Table 1**. For these 15 nsSNPs, predictions on functional impact and stability were performed using 10 different bioinformatic servers

Table 1. Prediction of 15 highly deleterious nsSNP found by SIFT and PolyPhen

Variation ID	Variant	Mutation	SIFT		Polyphen	
			Score	Prediction	Score	Prediction
rs1163858187	G/T	C70F	0	Deleterious	1	Probably Damaging
rs1446449750	C/A	L76I	0.01	Deleterious	1	Probably Damaging
rs149950065	C/A	A118E	0.01	Deleterious	1	Probably Damaging
rs778014138	G/A	R139W	0.01	Deleterious	0.996	Probably Damaging
rs199929962	T/C	M144T	0.03	Deleterious	0.994	Probably Damaging
rs1361163509	C/T	A94T	0.04	Deleterious	0.994	Probably Damaging
rs778014138	G/C	R139G	0.01	Deleterious	0.993	Probably Damaging
rs376367511	T/C	C123R	0	Deleterious	0.99	Probably Damaging
rs1444583505	T/C	L7P	0.02	Deleterious	0.983	Probably Damaging
rs149950065	C/G	A118G	0.02	Deleterious	0.979	Probably Damaging
rs775753738	C/T	L110F	0.01	Deleterious	0.975	Probably Damaging
rs753127489	C/A	S81I	0	Deleterious	0.95	Probably Damaging
rs751850550	G/A	R112C	0	Deleterious	0.941	Probably Damaging
rs1245723965	C/T	A58V	0.01	Deleterious	0.934	Probably Damaging
rs4252548	C/T	R112H	0.01	Deleterious	0.922	Probably Damaging

Furthermore, PolyPhen-2, PANTHER, and PredictSNP offer insights into the potential impact of mutations on IL4 protein function. Among the 15 nsSNPs analyzed, PANTHER predicted that 13 of these variants could be possibly damaging, while two (A94T and S81I) were classified as probably benign. PredictSNP results similarly identified A94T and S81I as neutral, with the remaining 13 nsSNPs likely to have deleterious effects. Moreover, PolyPhen-2 considered all 15 nsSNPs as probably damaging, as detailed in **Table 2**.

Table 2. Screening of functional impact of nsSNPs by PANTHER, PredictSNP & Polyphen2

Variation ID	Mutation	PANTHER		Predict SNP	Polyphen2
		Prediction	Score	Prediction	Prediction

rs1163858187	C70F	Possibly damaging	0.5	Deleterious	Probably Damaging
rs1446449750	L76I	Possibly damaging	0.5	Deleterious	Probably Damaging
rs149950065	A118E	Possibly damaging	0.5	Deleterious	Probably Damaging
rs778014138	R139W	Possibly damaging	0.5	Deleterious	Probably Damaging
rs199929962	M144T	Possibly damaging	0.5	Deleterious	Probably Damaging
rs1361163509	A94T	Probably benign	0.19	Neutral	Probably Damaging
rs778014138	R139G	Possibly damaging	0.5	Deleterious	Probably Damaging
rs376367511	C123R	Possibly damaging	0.5	Deleterious	Probably Damaging
rs1444583505	L7P	Possibly damaging	0.5	Deleterious	Probably Damaging
rs149950065	A118G	Possibly damaging	0.5	Deleterious	Probably Damaging
rs775753738	L110F	Possibly damaging	0.5	Deleterious	Probably Damaging
rs753127489	S81I	Probably benign	0.19	Neutral	Probably Damaging
rs751850550	R112C	Possibly damaging	0.5	Deleterious	Probably Damaging
rs1245723965	A58V	Possibly damaging	0.5	Deleterious	Probably Damaging
rs4252548	R112H	Possibly damaging	0.5	Deleterious	Probably Damaging

3.3. Functional nsSNPs with disease

According to **Table 3**, SNPs & GO predicted that 14 nsSNPs analyzed are associated with disease, with only the rs1361163509 (A94T) variant considered neutral. Meta SNP analysis identified 7 nsSNPs as neutral and classified 8 as disease-related. In contrast, SuSPect classified all 15 nsSNPs as disease-related.

Table 3. Findings of disease-linked nsSNPs and their effect on IL4 stability.

Variation ID	AA	Suspect	Meta SNP		SNP & Go		MUpro		i-stable	
		Sc	Effect	Sc	Sc	Effect	Stability	Detal Delta	Stability	Conf. score
rs1163858187	C70F	99	D	4	9	D	Decrease	-0.665856	Increase	0.232482
rs1446449750	L76I	84	D	2	6	D	Decrease	-0.600843	Decrease	-1
rs149950065	A118E	69	D	2	6	D	Decrease	-0.426898	Increase	0.314662
rs778014138	R139W	89	D	2	8	D	Decrease	-0.669057	Decrease	-1
rs199929962	M144T	92	D	3	9	D	Decrease	-1.643079	Decrease	-0.530474
rs1361163509	A94T	62	N	8	1	N	Decrease	-0.334169	Increase	0.317224
rs778014138	R139G	82	N	1	8	D	Decrease	-1.694123	Decrease	-1
rs376367511	C123R	98	D	6	10	D	Decrease	-1.854136	Decrease	-1
rs775753738	L110F	90	N	3	8	D	Decrease	-1.5245074	Increase	-1
rs1444583505	L7P	90	N	5	8	D	Decrease	-1.610338	Decrease	-1
rs753127489	S81I	56	N	7	3	D	Decrease	-0.508011	Decrease	-0.290899
rs751850550	R112C	87	D	5	9	D	Decrease	-0.779039	Decrease	-1
rs1245723965	A58V	59	N	6	6	D	Decrease	-0.0818102	Increase	0.558775
rs4252548	R112H	82	D	5	9	D	Decrease	-0.967623	Decrease	-0.77776
rs149950065	A118G	69	N	6	5	D	Decrease	-1.062422	Increase	0.433026

*** AA:** Amino Acid**; D:** Disease**; N:** Neutral**; Sc:** Score

3.4. Protein Stability change by variations

Using the MuPro server, all 15 nsSNPs were found to reduce protein stability. In this study, i-Stable predicts changes in protein thermal stability, rs1446449750 (L76I), rs778014138 (R139W), rs199929962 (M144T), rs778014138 (R139G), rs376367511 (C123R), rs1444583505 (L7P), rs753127489 (S81I), rs751850550 (R112C), and rs4252548 (R112H) decrease thermal stability. In contrast, rs63858187 (C70F), rs149950065 (A118E), rs1361163509 (A94T), rs149950065 (A118G), rs775753738 (L110F), and rs1245723965 (A58V) increase stability as summarized in **Table 3**.

3.5. Modeling of IL4 protein

The reported 3D model of the IL4 protein in the NCBI database is incomplete. To address this limitation, we used the Swiss Model server to generate a more comprehensive template. Our analysis focused on assessing structural changes in the IL4 protein induced by 15 highly conserved mutations. The Mutation 3D analysis revealed that the mutations A58V, R139G, R139W, and M144T are categorized as covered mutations, while A118G, C70F, L61I, A94T, L7P, L110F, S81I, R112C, R112H, and C123R are grouped as clustered mutations, as shown in **Table 4**. The 3D structures of these mutations are visualized with the mutations highlighted in red and blue, as depicted in **Figure 3**. These structural visualizations aid in understanding the spatial distribution and potential impact of the mutations on the IL-4 protein.

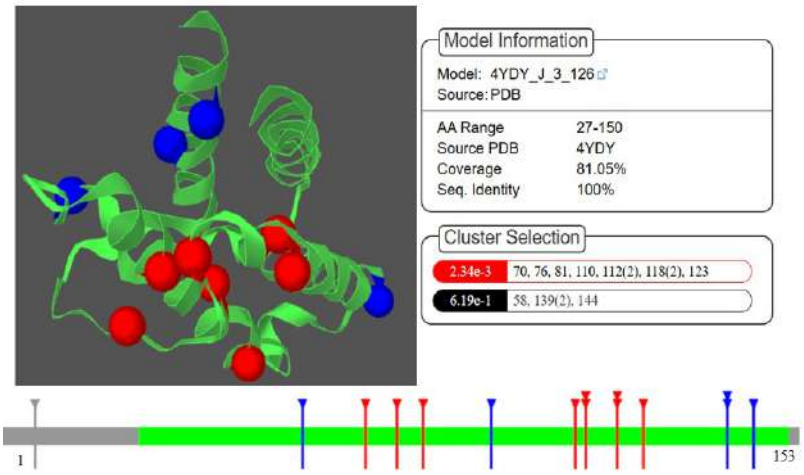

Figure 3. Visual representation of IL4 model by Mutation 3D.

Out of the 15 templates from SWISS-MODEL, 93.46% matched the STML ID P51492.1A. The IL-4 protein's three-dimensional structure was accurately modeled using the Alphafold DB model of IL4-MACMU (*Homo sapiens*) for the query sequence, with the template P51492.1A (amino acid range: 1-153) and are visualized using PyMOL, and the final model is presented in **Figure 4a**. This modeling method provides a comprehensive understanding of the structural alterations caused by mutations in the IL-4 protein. Our study was further used Galaxy Refine, which significantly improved the model quality and selected Model 05 as the refined version. The modeled framework was validated using SAVES v6.1, and the secondary structure was assessed through a RAMACHANDRAN plot evaluation. The final model met all criteria set forth by potential energy calculations. As shown in **Figure 4b**, 98.60% of the amino acid residues in the IL-4 protein were positioned in a favorable region on the RAMACHANDRAN plot, suggesting high structural integrity. All of the anticipated outcomes are summarized in **Table 4** and A118G, A139W, R112C, and R139G exhibit high RMSD values, indicating notable structural deviations.

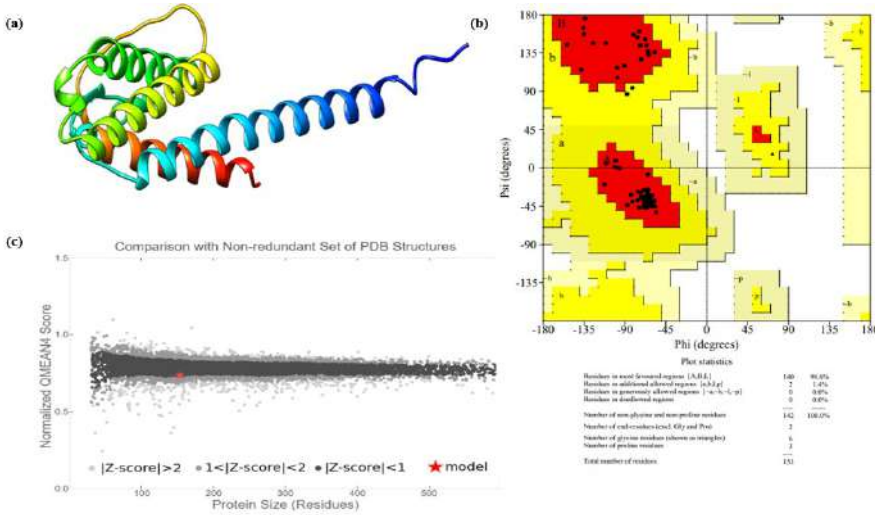

Figure 4. IL4 protein configuration (a) 3D IL4 Structure (b) Model Quality (c) Statistics of Ramachandran Plot

Moreover, QMEAN gives QMEAN Z-score of −0.81, which is comparable to experimental structures of similar sizes to predict model quality. A negative QMEAN Z-score indicates potential structural instability of the protein. As shown in **Figure 4c,** the IL-4 model is represented by a red star. All proteins on this list had their corresponding PDB files retrieved and modified using PyMOL.

Table 4. Prediction of variants effect and structure verification confirmation score

AA	Mutation 3D	ERRAT	Procheck				Verify	TM Align	
		Score	Core	Allow	Generously	Disallowed	Score	TM Sc	RMSD
Model		95.5882	97.90%	2.10%	0.00%	0.00%	64.05%		
C70F	Clustered	89.5105	97.90%	2.10%	0.00%	0.00%	65.36%	0.99538	0.32
L76I	Clustered	95.5882	97.90%	2.10%	0.00%	0.00%	63.40%	0.9961	0.29
A118E	Clustered	95.6835	97.90%	2.10%	0.00%	0.00%	64.05%	0.99594	0.3
R139W	Covered	95.5882	97.90%	2.10%	0.00%	0.00%	62.75%	0.99429	0.36
A94T	Clustered	95.5882	97.90%	2.10%	0.00%	0.00%	64.05%	0.99563	0.31
R139G	Covered	95.5882	97.90%	2.10%	0.00%	0.00%	64.05%	0.99284	0.41
C123R	Clustered	89.5105	97.90%	2.10%	0.00%	0.00%	59.48%	0.99509	0.33
L7P	Clustered	94.8905	97.90%	2.10%	0.00%	0.00%	64.05%	0.99604	0.29
A118G	Clustered	95.5882	97.90%	2.10%	0.00%	0.00%	64.05%	0.99496	0.34
L110F	Clustered	95.5882	97.90%	2.10%	0.00%	0.00%	64.05%	0.99592	0.3
S81I	Clustered	95.5882	97.90%	2.10%	0.00%	0.00%	64.05%	0.99510	0.33
R112C	Clustered	95.5882	97.90%	2.10%	0.00%	0.00%	64.05%	0.99443	0.35
A58V	Covered	95.5882	97.90%	2.10%	0.00%	0.00%	59.48%	0.99563	0.31
R112H	Clustered	95.5882	97.90%	2.10%	0.00%	0.00%	64.05%	0.99551	0.31
M144T	Covered	95.5882	97.90%	2.10%	0.00%	0.00%	64.05%	0.99557	0.31

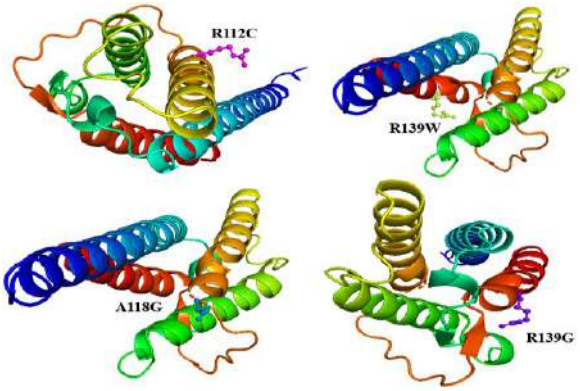

Figure 5. Structure of mutant IL4 protein visualized by PyMOL Program

3.6. Protein-Ligand Docking Analysis

In the present study, we docked 25 selected ligands from PubChem with both the wild-type and mutant (R139W, R139G, A118G, and R112C as given in **Figure 5**) forms of the IL-4 protein using the PyRx program to explore ligand-protein interactions. For each ligand, 10 unique conformations were generated, with binding affinities reported in -Kcal/mol. The docking results reveal a correlation between binding affinity and ligand activity, highlighting the

effectiveness of specific compounds in interacting with IL-4 and its variants.

Table 5. Docking score of 25 ligands with wild-type and mutant *IL-4* proteins.

Ligands	P51492.1A	R139W	R139G	A118G	R112C
Apigenin	-6.4	-6.4	-6.3	-6.3	-6.4
Benazepril	-5.6	-5.7	-5.6	-5.6	-5.7
Enalapril	-5.2	-5.1	-5.8	-5.5	-5.6
GAG	-4.5	-4.5	-4.5	-4.5	-4.5
GN8	-6.5	-6.5	-6.5	-6.5	-6.5
Ioniflavone	-8.3	-8.3	-8.2	-8.3	-8.3
Meridine	-7.4	-7.4	-7.4	-6.7	-7.3
Meoxipril	-5.5	-5.7	-5.7	-5.7	-5.7
Palbociclib	-7.0	-7.0	-7.0	-7.0	-7.0
Pyranoamentoflavone	-8.2	-8.2	-6.9	-8.2	-8.2
Quinapril	-5.7	-5.7	-5.9	-5.7	-5.7
Ramipril	-6.0	-6.1	-6.8	-6.2	-6.3
Riluzole	-5.6	-5.6	-5.4	-5.6	-5.6
Refecoxib	-5.9	-5.9	-6.0	-5.8	-5.9
S-Adenosylmethionine	-5.6	-5.9	-5.5	-5.8	-5.8
Saxitoxin	-6.4	-6.3	-6.5	-6.4	-6.3
Sclareol	-5.8	-5.9	-5.8	-5.9	-5.8
Sinularin	-6.2	-6.3	-6.3	-6.1	-6.3
Tamoxifen	-5.4	-5.4	-5.7	-5.9	-5.6
Tetracycline	-7.6	-7.5	-5.4	-7.3	-7.5
Tetrodotoxin	-6.4	-6.4	-5.5	-6.4	-6.4
Thymoquinone	-5.4	-5.0	-5.3	-4.8	-5.4
Topiramate	-5.9	-5.9	-6.0	-6.0	-6.0
Trandolapril	-6.4	-6.3	-6.4	-6.4	-6.2
Vixotrigine	-6.7	-6.4	-6.3	-6.6	-6.6

Our study on IL-4 interactions with various ligands has identified several compounds with promising therapeutic potential for conjunctivitis by targeting inflammation and infection pathways. The study highlighted five compounds Ioniflavone, Meridine, Pyranoamentoflavone, Palbociclib, Tetracycline, and Ramipril that demonstrated substantial binding affinities when docked with both the native IL-4 protein and its mutant complexes. The binding affinity scores ranged from -4.5 Kcal/mol to -8.3 Kcal/mol, as shown in **Table 5**. These findings underscore the potential of these compounds in effectively interacting with IL-4 and its mutant forms, suggesting promising candidates to treat eye infections (conjunctivitis). Using Discovery Studio, we visualized and predicted the interactions between each ligand and the active site of the IL-4 protein, illustrating key binding interactions and affinities as given in **Figure 6**. This visualization provides insight into the binding mechanisms and structural compatibility of each compound, supporting their potential efficacy as inhibitors or modulators of the IL-4 protein.

In **Table 6**, the IL-4 binding pocket was filled with the ligand Ioniflavone, which exhibited significant interactions with key residues through Van der Waals forces. The involved residues include TYR80, ARG77, VAL75, VAL53, THR49, LEU103, GLU134, PHE106, ASN39, SER40, ARG109, ARG112, ILE35, THR42, LYS141, GLN32, LEU31, THR30, and ILE29. Ioniflavone, a flavonoid known for its anti-inflammatory and antioxidant properties, has the potential to reduce inflammation and oxidative stress. Given these attributes, it may help alleviate conjunctivitis symptoms by modulating immune response, underscoring its potential as a therapeutic agent in treating eye infections. The docking studies revealed that the Meridine and Palbociclib ligands have strong binding affinities with IL-4 binding pocket, with several key interactions that suggest therapeutic potential in inflammation-related eye conditions as shown in **Figure 6**.

Moreover, Meridine showed binding through Van der Waals interactions with residues such as LEU133, THR42, ASN39, LYS141, LYS36, ILE35, GLU33, ASP111, ARG109, PHE106, and LEU114, showcases anti-inflammatory properties that may help reduce swelling and discomfort in conjunctivitis by modulating inflammatory pathways. Similarly, Palbociclib interacted with native IL-4 binding pocket residues ILE29, LEU31, GLN32, LYS36, ASN39, ILE35, ARG109, THR42, LEU140, ALA73, ARG112, LYS108, PHE106, PHE136, and LEU103 as summarized in **Table 6**. Although Palbociclib is primarily known as a cell cycle modulator in cancer treatments, its role in reducing immune cell proliferation could help control excessive inflammatory responses in conjunctivitis.

Moreover, Pyranoamentoflavone displayed favorable binding within the native IL-4 binding pocket, involving interactions with residues such as ALA72, LYS108, ARG77, TRP115, TYR80, and LEU133 as shown in **Table 6**. By inhibiting microbial growth, Pyranoamentoflavone could reduce the bacterial or viral load associated with eye infections, while its anti-inflammatory effects may alleviate symptoms and prevent tissue damage due to prolonged inflammation. Tetracycline formed interactions with several native IL-4 residues, including PHE136, LEU133, LEU107, THR42, LEU140, and LYS141 as given in **Table 6**. Known for its effectiveness against bacterial infections, it operates by blocking bacterial protein synthesis, as it allows for the rapid reduction of the infection, promoting tissue healing and reducing the risk of secondary complications. Lastly, Ramipril is typically used as an ACE inhibitor, its ability to modulate inflammation could make it a valuable adjunct treatment for conjunctivitis characterized by significant inflammatory responses. Moreover, mutant IL4 proteins (A118G, A139W, R112C, and R139G) highlighted the active site residues as summarized in **Table 6**.

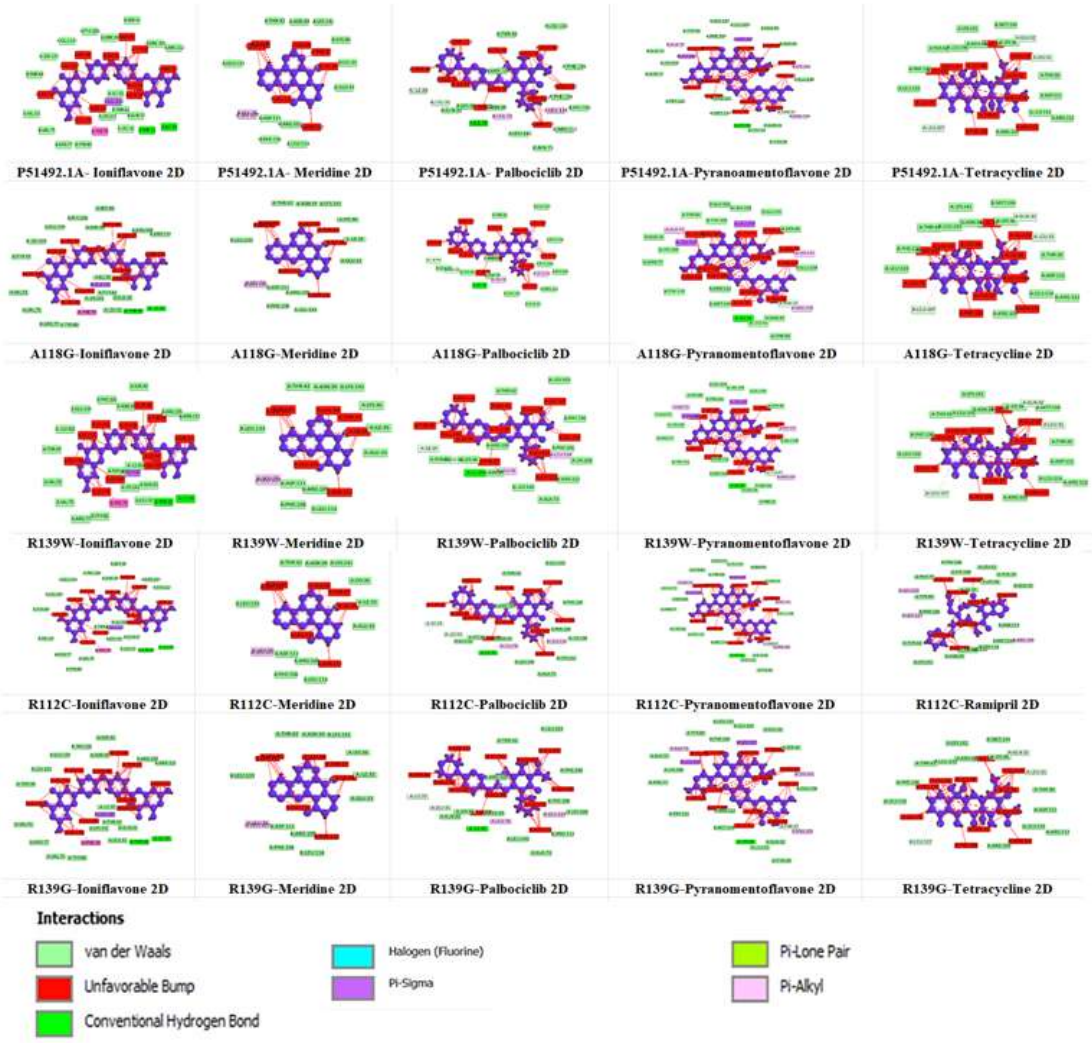

Figure 5. IL4 protein with ligands show 2D interactions visualization by Discovery Studio Visualizer

These compounds present a promising range of therapeutic actions for conjunctivitis, addressing both infectious and immune-related factors. Their diverse mechanisms antimicrobial, anti-inflammatory, and immune-modulating could potentially improve the management of conjunctivitis, especially in complex cases with bacterial, viral, or inflammatory components. Future pharmacological and clinical investigations will be crucial to confirm their suitability for ophthalmic use, as well as to determine optimal dosing and safety profiles.

Table 6. Interacting active residues of IL4 protein with ligands obtained from docking studies

Protein-Ligands	Hydrophilic interactions	Hydrophobic interactions	Stearic Hinderance
P51492.1A-Ioniflavone	TYR80,ARG77,VAL75,VAL53,THR49, LEU103,GLU134, PHE106, ASN39, SER40, ARG109, ARG112, ILE35, THR42, LYS141, GLN32, LEU31, THR30, ILE29	LEU110, PHE79	ASN113, THR37, IL334, GLU33, LYS36, LEU38, LEU41, LEU137, LEU133, LEU107, LEU76
P51492.1A-Meridine	LEU133, THR42, ASN39, LYS141, LYS36, ILE35, GLU33, ASP111, ARG109, PHE106, LEU114	LEU76, LEU107	LEU41, LEU137,LEU38, LEU110, THR37, ILE34, ASN113
P51492.1A-Palbociclib	ILE29, LEU31, GLN32, LYS36, ASN39, ILE35, ARG109, THR42, LEU140, ALA73, ARG112, LYS108, PHE106, PHE136, LEU103	LEU76, LEU114	THR30, ASN113, GLU33, ILE34, THR37, LEU38, LEU41, LEU137, LEU107, LEU110, ASP111, LEU133
P51492.1A-Pyranoamentoflavone	ALA72, LYS108, ARG77, TRP115, TYR80, LEU133, PHE106, LEU103, GLU43, SER40, ARG112, MET144, LYS36, LEU31, GLN32, THR30,THR37 GLU138	ALA73, LEU114, LEU137, LYS141, ARG109	LEU76, LEU107, LEU110, ASP111, LEU140, LEU41, THR42, LEU38, ASN39, ASN113, ILE34, ILE35, GLU33
P51492.1A-Tetracycline	PHE136, LEU133, LEU107, THR42, LEU140, LYS141, ASN39, MET144, GLN32, LEU31, THR30, ASP111, LEU114, ARG112, ARG109, LYS36	NULL	LEU76, LEU137, LEU41, LEU38, ILE35, GLU33, ILE34, LEU110, THR37, PHE106, ASN113
A118G-Ioniflavone	THR49, VAL53, LEU103, VAL75, ARG77, GLU134, PHE106, ASN39, SER40, ARG109, ARG112, ILE35, THR42, LYS141, GLN32, TYR80, LEU31, THR30, ILE29	LEU110, PHE79	LEU133, LEU137, LEU41, LEU107, LEU76, LEU38, LYS36, THR37, ILE34, GLU33, ASN113
A118G-Meridine	LEU133, THR42, ASN39, LYS141, LYS36, ILE35, GLU33, ASP111, ARG109, PHE106, LEU114	LEU76, LEU107	LEU41, LEU137, LEU38, THR37, ILE34, LEU110, ASN113
A118G-Palbociclib	ILE29, GLN32, LEU31, LYS36, ILE35, ASN39, THR42, LEU140, ALA73, ARG112, LYS108, PHE106, PHE103, PHE136, LEU103	LEU76, LEU114	THR30, ASN113, GLU33, ILE34, LEU41, THR37, LEU137, LEU107, LEU133, LEU10, ASP111
A118G-Pyranoamentoflavone	ARG77, ALA72, LYS108, TYR80, TRP115, PHE106, LEU133, LEU103, GLU43, SER40, GLU138, THR37, GLN32, THR30, LEU31, LYS36, MET144, ARG112	ALA73, LEU114, LEU137, LYS141, ARG109	LEU76, LEU107, LEU110, ASP111, LEU140, LEU41, THR42, LEU38, ASN39, ASN113, ILE34, ILE35, GLU33
A118G-Tetracycline	LEU133, PHE136,THR42, LEU140, LYS141, ASN39, MET144, LYS36, GLN32, LEU31, THR30, ASP111, LEU114, ARG112, ARG109, LEU107	NULL	LEU76, LEU137, LEU41, LEU38, ILE35, GLU33, ILE34, LEU110, THR37, PHE106, ASN113
R139W-Ioniflavone	TYR80, ARG77, VAL75, VAL53, THR49, LEU103, GLU134, PHE106, ASN39, SER40, ARG109, ARG112,	LEU110, PHE79	LEU133, LEU137, LEU41, LEU107, LEU76, LEU38,

	ILE35, THR42, LYS141, GLN32, LEU31, THR30, ILE29		LYS36, THR37, ILE34, GLU33, ASN113
R139W-Meridine	LEU133, THR42, ASN39, LYS141, LYS36, ILE35, GLU33, ASP111, ARG109, PHE106, LEU114	LEU76, LEU107	LEU41, LEU137, LEU38, THR37, ILE34, LEU110, ASN113
R139W-Palbociclib	ILE29, GLN32, LEU31, LYS36, ILE35, ASN39, ARG109, THR42, LEU103, PHE136, PHE106, LYS108, ARG112, LEU140, ALA73	LEU114, LEU76	LEU137, LEU107, LEU133, LEU110, ASP111, LEU41, LEU38, THR37, ASN113, GLU33, ILE34, THR30
R139W-Pyranoamentoflavone	ALA72, LYS108, ARG77, TRP115, TYR80, LEU133, LEU103, GLU43, SER40, GLU138, ARG112, MET144, LYS36, LEU31, GLN32, THR37, THR30, PHE106	ALA73, LEU114, LEU137, LYS141, ARG109,	LEU76, LEU107, LEU110, ASP111, LEU140, BLEU41, THR42, LEU38, ASN39, ASN113, ILE34, GLU33, ILE35
R139W-Tetracycline	LEU133, PHE136, THR42, LEU107, LEU140, LYS141, ASN39, LYS36, GLN32, MET144, LEU31, THR30, ASP111, LEU114, ARG112, ARG109,	NULL	LEU76, LEU137, LEU41, LEU38, ILE35, GLU33, ILE34, LEU110, THR37, PHE106, ASN113
R112C-Ioniflavone	THR49, GLU134, LEU103, VAL53, ARG77, TYR80, VAL75, PHE106, SER40, ASN39, ARG109, CYS112, THR42, ILE35, LYS141, GLN32, LEU31, THR30, ILE29	LEU110, PHE79	LEU41, LEU137, LEU133, LEU76, LEU107, LEU38, LYS36, THR37, ILE34, GLU33, ASN113
R112C-Meridine	LEU133, THR42, ASN39, LYS141, LYS36, ILE35, GLU33, ASP111, ARG109, PHE106, LEU114	LEU76, LEU107	LEU41, LEU137, LEU38, THR37, ILE34, LEU110, ASN113
R112C-Palbociclib	ILE29, LEU31, LYS36, GLN32, ASN39, ILE35, LEU140, ALA73, CYS112, LYS108, PHE106, PHE136, LEU103, THR42, ARG109	LEU76, LEU114	THR30, ASN113, GLU33, ILE34, THR37, LEU41, LEU38,LEU107, LEU137, LEU133, LEU110, ASP111
R112C-Pyranoamentoflavone	ALA72, LYS108, ARG77, TRP115, CYS112, MET144, LYS36, LEU31, GLN32, LEU31, THR30, THR37, GLU138, SER40, GLU43, LEU103, LEU133, PHE106, TYR80	ALA73, LEU114, LEU137, LYS141, ARG109	THR42, ASN39, ASN113, GLU33, LEU41, LEU38, ILE34, ILE35, LEU76, LEU107, LEU110, ASP111, LEU140
R112C-Ramipril	PHE79, TYR80, PHE106, THR42, LYS141, PHE136, LYS108, ILE35, LEU31, THR30, LYS36, GLN32, ASN113, MET144, LEU114, ASP111, LEU140, ASN39	LEU133, LEU137, ARG109	LEU76, THR37, LEU107, ILE34, GLU33, LEU110, LEU38, LEU41
R139G-Ioniflavone	TYR80, VAL75, ARG77, VAL53, THR49, LEU103, GLU134, PHE106, ASN39, SER40, ARG109, ARG112, ILE35, THR42, LYS141, GLN32, LEU31, THR30, ILE30	LEU110, PHE79	ASN113, LYS36, THR37, ILE34, GLU33, LEU38, LEU41, LEU137, LEU107, LEU76, LEU133
R139G-Meridine	LYS36, ILE35, GLU33, LYS141, ASN39, THR42, LEU133, ASP111, ARG109, PHE106, LEU114	LEU76, LEU107	LEU41, LEU137, LEU38, LEU110, THR37, ILE34, ASN113
R139G-Palbociclib	LEU103, PHE136, PHE106, LYS108, ARG112, ALA73, THR42, ARG109, ASN39, LEU140, ILE35, LYS36, GLN32, LEU31, ILE29	LEU114, LEU76,	LEU107, LEU137, LEU133, LEU110, ASP111, ASN113, LEU41, GLU33, ILE34, LEU38, THR37, THR30
R139G-Pyranoamentoflavone	TYR80, ALA72, LYS108, ARG77, TRP115, LEU133, LEU103, PHE106, GLU43, SER40, GLU138, THR37,	ALA73, LEU114, LEU137, LYS141, ARG109	LEU76, LEU107, LEU110, ASP111, LEU140, LEU41, THR42, ASN39, LEU38,

	GLN32, LYS36, LEU31, THR30, ARG112, MET144		ASN113, ILE34, GLU33, ILE35
R139G-Tetracycline	LEU140, THR42, PHE136, LEU133, LEU107, LYS141, ASN39, MET144, LYS36, GLN32, LEU31, THR30, ASP111, LEU114, ARG112, ARG109,	NULL	GLU33, ILE34, LEU110, ASN113, ILE35, LEU38, THR37, PHE106, LEU41, LEU137, LEU76

3.7. Mutational effect on IL4 protein

The HOPE server analysis hypothesized that altering a single amino acid in the IL-4 protein would significantly affect its structural and functional properties, including spatial arrangement, hydrophobicity, and both physical and chemical characteristics. We found the substitution of amino acid R139W results in a larger mutant compared to the wild-type residue, whereas the mutations R112C, R139G, and A118G lead to smaller variants as given in **Table 7**. In addition, R139W, R112C, R139G, and A118G show increased hydrophobicity, which may alter interactions within the protein structure and potentially affect protein folding. The analysis further suggests that the mutations R112C, R139G, and A118G are possibly damaging to the protein's stability and function. These structural changes in key regions could thus have significant implications for the IL-4 protein's biological function, potentially impacting immune signalling pathways.

Table 7. Physiochemical properties of mutant IL4 protein by HOPE Project

rsID	Mutations	Mutant a.a size	SNP Location	Polymorphism	Amino acid properties
rs778014138	R139W	Bigger	More hydrophobic	NULL	Wild-type residue is lost by this mutation. This can cause loss of interactions with other molecules.
rs751850550	R112C	Smaller	More hydrophobic	Possibly Damaging	The mutant residue is smaller than the wild-type residue. This will cause a possible loss of external interactions.
rs778014138	R139G	Smaller	More hydrophobic	Possibly Damaging	The charge of the wild-type residue is lost by this mutation. This can cause loss of interactions with other molecules.
rs149950065	A118G	Smaller	More hydrophobic	Possibly Damaging	The mutant residue is smaller than the wild-type residue. The mutation will cause a space in the core of the protein.

DISCUSSION

The current study comprehensively analyzed the data on disease-causing nonsynonymous single nucleotide polymorphisms (nsSNPs) in the IL-4 gene using several prediction tools, including SIFT, PolyPhen, PANTHER, PolyPhen2, SUSPECT P, MetaSNPs, MuPro, SNP&GO, iStable, and Predict SNP. Bioinformatics tools have been employed to predict the functional consequences of mutations in the IL-4 gene, revealing how changes in its structure and stability may influence disease outcomes. The IL-4 protein's role in immune modulation is further highlighted by its effect on macrophage activation, where IL-4 induces M2 polarization, promoting tissue repair and regulating inflammation. Interleukin-4 (IL-4) plays a pivotal role in the immune system, particularly in the regulation of humoral immunity and allergic responses. It influences the differentiation of naive T cells into Th2 cells and enhances B-cell differentiation, promoting IgE production, which is crucial in allergic reactions. IL-4's effect on immune responses makes it essential in managing conditions like asthma, rheumatoid arthritis, and allergic conjunctivitis, where it drives inflammation in response to allergens or infections.

In conjunctivitis, IL-4 levels are elevated in patients with seasonal allergic conjunctivitis and vernal keratoconjunctivitis, reflecting its significant involvement in these allergic eye diseases. The gene encoding IL-4, located on chromosome 5q31-q33, undergoes various genetic mutations that affect its expression, influencing susceptibility to eye infections, especially viral conjunctivitis. For instance, the c.-589C>T polymorphism has been linked to altered IL-4 expression, potentially heightening susceptibility to infections like viral

conjunctivitis, while the IL-4 receptor variant rs1805010 showed no significant association with the condition. These genetic variations underscore the impact of IL-4 in immune dysregulation and disease susceptibility. These tools helped assess the potentially detrimental effects of 15 known nsSNPs on IL-4 function and protein stability.

The PANTHER analysis identified 13 nsSNPs as potentially harmful, while two variants, A94T and S81I, were likely benign. Predict SNP similarly predicted a neutral effect for A94T and S81I, whereas PolyPhen2 classified all 15 nsSNPs as possibly damaging. Additionally, SNP&GO, SuSpect, and MetaSNP identified several of these nsSNPs as linked to disease prediction. To understand the impact on protein stability, iStable and MuPro were employed. MuPro's analysis indicated a decrease in stability for all 15 nsSNPs, whereas iStable revealed that 9 nsSNPs caused a reduction in thermal stability, with the remaining 6 leading to stability increases. Mutation 3D mapping revealed that of these 15 mutations, 6 were mapped, 8 were clustered, and 1 remained unmapped. This analysis helped to refine understanding of the functional and structural impacts of these mutations.

Moreover, Structural assessment was performed using SWISS-MODEL, PROCHECK, QMEAN, ERRAT, verify 3D, and TM-Align, which together confirmed the model's high-quality structure for the IL-4 protein sequence. Notably, the Ramachandran plot demonstrated the stereochemical quality of the modeled protein, with more than 90% of residues in preferred regions. SWISS-MODEL confirmed sequence conservation within the amino acid range of 1–153, and QMEAN-Z scores validated the model's quality. Molecular docking studies were conducted using PyRx Autodock Vina to assess the binding affinities of 25 ligands with both normal and mutated IL-4 complexes. Key findings included high docking scores for the interactions between the IL-4 model and several ligands, Ioniflavone (-8.3), Meridine (-7.4), Palbociclib (-7.0), Pyranoamentoflavone (-8.2), and Tetracycline (-7.6). Visualization of these interactions with Discovery Studio Visualizer provided insights into ligand binding within the IL-4 binding pocket, highlighting the potential for therapeutic applications of these compounds.

The evolutionary conservation profile indicated that deleterious nsSNPs tended to be located in conserved regions, further underscoring their potential impact on protein function. Using HOPE, we identified the four most detrimental mutations R139G, A118G, R112C, and R139W and analyzed their predicted effects on IL-4 structure, noting that R139W was larger than the wild type, while the other three were smaller. These mutations were found within critical domains, suggesting they may disrupt IL-4's immune regulatory function. Studies by Gu et al. (2020) and Wei et al. (2017) have shown that compounds targeting IL-4 pathways could help mitigate the inflammatory response in diseases such as conjunctivitis. The use of tools like HOPE to evaluate the structural consequences of mutations further builds on the growing body of literature that integrates computational biology with experimental methods to elucidate the functional effects of mutations.

By identifying key regions of IL-4 affected by deleterious mutations, this study contributes to our understanding of how genetic variations influence immune function and supports the development of targeted therapies for IL-4-associated diseases, underscoring the importance of computational tools in modern drug development. This study underscores the need for further research on the pathogenicity, stability, and functional implications of nsSNPs in IL-4, with potential applications in treating conjunctivitis. In clinical settings, genetic testing and in silico analysis could guide treatment decisions, especially in the context of immune modulation, where IL-4 plays a key role in allergic infection. Advancing our understanding of nsSNPs and integrating computational and laboratory-based approaches could pave the way for new therapeutic targets and personalized medicine strategies for IL-4-associated diseases. The ultimate aim is to improve health outcomes and quality of life for patients with IL-4-related immune disorders through a collaborative effort among computational biologists, clinicians, and the pharmaceutical industry.

CONCLUSION

Using in-silico tools, 15 potentially damaging SNPs were identified, with variants like R139G, A118G, R112C, and R139W showing significant structural damage and altered protein stability, as indicated by high RMSD values and SAVESV6.1 analysis. Structural modeling using HOPE revealed that R139W might disrupt the IL-4 protein's structure, potentially making it larger than the wild type.

Molecular docking studies identified several compounds, including Ioniflavone, Meridine, and Tetracycline, as having strong binding affinities to IL-4, suggesting potential therapeutic benefits. These findings highlight the significance of IL-4 genetic variants in influencing pink eye susceptibility and pave the way for future targeted therapies. However, further clinical studies are needed to assess the efficacy and safety of these compounds in treating ocular inflammation based on IL-4 genetic profiles. This study provides valuable insights for future experimental research and therapeutic approaches for immune-related diseases, including conjunctivitis.

ACKNOWLEDGMENTS

Not applicable

Author contribution

Not applicable

Funding statement

No Funding

Data Availability

The NCBI database (https://www.ncbi.nlm.nih.gov/search/all/?term=dbSNP) now contains publicly available data that was collected or analyzed during this study.

Competing interests

No conflicts of interest.

REFERENCE

1. Flajnik, M., Paul's fundamental immunology. 2022: Lippincott Williams & Wilkins.
2. Abraha, R., Review on the role and biology of cytokines in adaptive and innate immune system. Arch Vet Anim Sci, 2020. 2: p. 2.
3. Said, N., R. Fekry, and H. Elmesallmy, Association between viral Conjunctivitis and Genetic Polymorphisms related to IL-4 and IL-4R in Egyptian Population. Zagazig University Medical Journal, 2022. 28(6.2): p. 333-338.
4. Fujishima, H., et al., Measurement of IL-4 in tears of patients with seasonal allergic conjunctivitis and vernal keratoconjunctivitis. Clin Exp Immunol, 1995. 102(2): p. 395-8.
5. Schwartz, G.S., Around the eye in 365 days. 2024: CRC Press.
6. Azari, A.A. and A. Arabi, Conjunctivitis: a systematic review. Journal of ophthalmic & vision research, 2020. 15(3): p. 372.
7. Hu, Y.-L., et al., Predominant role of Haemophilus influenzae in the association of conjunctivitis, acute otitis media and acute bacterial paranasal sinusitis in children. Scientific Reports, 2021. 11(1): p. 11.
8. Rietveld, R.P., et al., Diagnostic impact of signs and symptoms in acute infectious conjunctivitis: systematic literature search. Bmj, 2003. 327(7418): p. 789.
9. Bielory, L., et al., ICON: diagnosis and management of allergic conjunctivitis. Annals of Allergy, Asthma & Immunology, 2020. 124(2): p. 118-134.
10. Berger, W.E., D.B. Granet, and A.G. Kabat. Diagnosis and management of allergic conjunctivitis in pediatric patients. in Allergy & Asthma Proceedings. 2017.
11. Vernhardsdottir, R.R., et al., Antibiotic treatment for dry eye disease related to meibomian gland dysfunction and blepharitis–A review. The ocular surface, 2022. 26: p. 211-221.
12. Haddad, E.-B., et al., Current and Emerging Strategies to Inhibit Type 2 Inflammation in Atopic Dermatitis. Dermatology and Therapy, 2022. 12(7): p. 1501-1533.
13. Choi, P. and H. Reiser, IL-4: role in disease and regulation of production. Clin Exp Immunol, 1998. 113(3): p. 317-9.
14. Paffen, E., et al., The− 589C> T polymorphism in the interleukin-4 gene (IL-4) is associated with a reduced risk of myocardial infarction in young individuals. Journal of Thrombosis and Haemostasis, 2008. 6(10): p. 1633-1638.
15. Howard, M. and W.E. Paul, Interleukins for B lymphocytes. Lymphokine research, 1982. 1(1): p. 1-4.
16. Yokota, T., et al., Isolation and characterization of a human interleukin cDNA clone, homologous to mouse B-cell stimulatory factor 1, that expresses B-cell-and T-cell-stimulating activities. Proceedings of the National Academy of Sciences, 1986. 83(16): p. 5894-5898.
17. Hasnain, M.J.U., et al., Computational analysis of functional single nucleotide polymorphisms associated with SLC26A4 gene. PLoS One, 2020. 15(1): p. e0225368.
18. Kuru, N., et al., PHACT: Phylogeny-aware computing of tolerance for missense mutations. Molecular Biology and Evolution, 2022. 39(6): p. msac114.
19. Chelbi, N.E., D. Gingras, and C. Sauvageau, Worst-case scenarios identification approach for

the evaluation of advanced driver assistance systems in intelligent/autonomous vehicles under multiple conditions. Journal of Intelligent Transportation Systems, 2022. 26(3): p. 284-310.
20. Ahmad, H.I., et al., [Retracted] Computational Insights into the Structural and Functional Impacts of nsSNPs of Bone Morphogenetic Proteins. BioMed Research International, 2022. 2022(1): p. 4013729.
21. Wanarase, S.R., S.V. Chavan, and S. Sharma, Evaluation of SNPs from human IGFBP6 associated with gene expression: an in-silico study. Journal of Biomolecular Structure and Dynamics, 2023. 41(23): p. 13937-13949.
22. Halder, S.K., et al., Identification of the most damaging nsSNPs in the human CFL1 gene and their functional and structural impacts on cofilin-1 protein. Gene, 2022. 819: p. 146206.
23. Sukumar, S., A. Krishnan, and S. Banerjee, An overview of bioinformatics resources for SNP analysis. Advances in bioinformatics, 2021: p. 113-135.
24. Chen, Z., et al., PhenoApt leverages clinical expertise to prioritize candidate genes via machine learning. The American Journal of Human Genetics, 2022. 109(2): p. 270-281.
25. Chen, C.-W., et al., iStable 2.0: Predicting protein thermal stability changes by integrating various characteristic modules. Computational and structural biotechnology journal, 2020. 18: p. 622-630.
26. Marabotti, A., B. Scafuri, and A. Facchiano, Predicting the stability of mutant proteins by computational approaches: an overview. Briefings in Bioinformatics, 2021. 22(3): p. bbaa074.
27. Tredennick, A.T., et al., A practical guide to selecting models for exploration, inference, and prediction in ecology. Ecology, 2021. 102(6): p. e03336.
28. Pan, A., G. Pranavathiyani, and S.S. Chakraborty, Computational Modeling of Protein Three-Dimensional Structure: Methods and Resources, in Molecular Docking for Computer-Aided Drug Design. 2021, Elsevier. p. 155-178.
29. Agnihotry, S., et al., Protein structure prediction, in Bioinformatics. 2022, Elsevier. p. 177-188.
30. Romano Spica, V., et al., In Silico Predicting the Presence of the S100B Motif in Edible Plants and Detecting Its Immunoreactive Materials: Perspectives for Functional Foods, Dietary Supplements and Phytotherapies. International Journal of Molecular Sciences, 2024. 25(18): p. 9813.
31. Kagami, L.P., et al., Geo-Measures: A PyMOL plugin for protein structure ensembles analysis. Computational Biology and Chemistry, 2020. 87: p. 107322.
32. Burley, S.K., et al., RCSB Protein Data Bank: Sustaining a living digital data resource that enables breakthroughs in scientific research and biomedical education. Protein Science, 2018. 27(1): p. 316-330.
33. Das, K.K., S. Pattnaik, and S.K. Behera, LOVASTATIN: AN ANTIVIRAL DRUG DESIGN APPROACH FOR CANCER AND COVID-19. 2024.
34. Mun, C.S., et al., Multi-targeted molecular docking, pharmacokinetics, and drug-likeness evaluation of coumarin based compounds targeting proteins involved in development of COVID-19. Saudi J Biol Sci, 2022. 29(12): p. 103458.
35. Haque, A., et al., Interaction Analysis of MRP1 with Anticancer Drugs Used in Ovarian Cancer: In Silico Approach. Life, 2022. 12(3): p. 383.
36. Roy, A.S., et al., A computational approach for structural and functional analyses of disease-associated mutations in the human CYLD gene. Genomics and Informatics, 2024. 22(1): p. 4.
37. Avery, C., et al., Protein function analysis through machine learning. Biomolecules, 2022. 12(9): p. 1246.

HOW TO CITE: Hamna Tariq*, Aniqa Amir, Muhammad Saleem, Kainat Ramzan*, Tuba Aslam, Mehmooda Asif, In-Depth In-Silico Functional, And Structural Screening Of IL-4 Gene Variants Linked with Pink Eye Infection, Int. J. Sci. R. Tech., 2024, 1 (11), 213-229. https://doi.org/10.5281/zenodo.14234050